Ocean Wave Measurement Using GPS Buoys

Research Article

G. Joodaki[1]*, H. Nahavandchi[1 †], K. Cheng[2 ‡]

1 Division of Geomatics, Norwegian University of Science and Technology, N-7491 Trondheim, Norway
2 Department of Earth and Environmental Sciences, National Chung Cheng University, 168 University Road, Minhsiung Township, Chiayi 62102, Taiwan

Abstract:
The observation of ocean wave parameters is necessary to improve forecasts of ocean wave conditions. In this paper, we investigate the viability of using a single GPS receiver to measure ocean-surface waves, and present a method to enhance the accuracy of the estimated wave parameters. The application of high-pass filtering to GPS data in conjunction with directional wave spectral theory is a core concept in this article. Laboratory experiments were conducted to test the viability and accuracy measurements of wave parameters made by a single GPS receiver buoy. These tests identified an error of less than 1% for the rotational arm measurement (wave height) and an error of 1% in verifications of the wave direction and wave period, and showed a 0.488 s bias; this is sufficiently accurate for many specific purposes. These results are based on the best cut-off frequency value derived in this study. A moored-sea GPS buoy on the Taiwanese coast was used to estimate the GPS-derived wave parameters. Our results indicate that data from a single GPS receiver, processed with the presented method to reduce the error of the estimated parameters, can provide measurements of ocean surface wave to reasonable accuracy.

1. Introduction

Accurate forecasts of wave conditions are of the utmost importance to everyone living, working, or traveling on or near the ocean. To improve wave prediction models, field measurement of wave height, period, and direction are necessary. Several devices exist to measure these parameters of an ocean wave, with ultrasonic sensors and accelerometers being the traditional tools. An ultrasonic sensor measures the distance to the surface of the sea from an observation device anchored on the sea floor through the emission, reflection, and detection of ultrasonic waves. The maximum measurable distance for ultrasonic sensors is around 50 m, so they cannot function in the ocean, and instead are useful only in littoral

areas. In contrast, an accelerometer measures wave height, period and direction by detecting the horizontal and vertical motions of the buoy, and is not restricted by deployment location. However, the cost of an accelerometer is generally high. A cheaper alternative to an accelerometer is a GPS-based wave buoy. Although GPS positioning at sea is common practice in navigation and even buoy monitoring, GPS wave measurement is still rare.

Several studies on GPS wave measurement exist in the literature. Krogstad et al. (1999) used differential GPS method (DGPS) to measure buoy velocities in north, east and vertical directions. Their results show that GPS-based wave buoys are more robust than conventional accelerometer-based wave sensors due to the fact that it has no moving parts, and because they are easier to deploy and transport. Jeans et al. (2003) showed that GPS-based buoys from Datawell (a private company that develops and produces oceanographic measurement instruments) have similar capabilities to accelerometer-based buoys. De Vries et al. (2003) addressed a new Datawell single-GPS way buoy, and computed the

*E-mail: gholamreza.joodaki@ntnu.no
† E-mail: Hossein.Nahavandchi@ntnu.no
‡ E-mail: cheng.168@ccu.edu.tw

VERSITA

velocity of the buoy in three dimensions using Doppler shifts in the frequencies of GPS signals. Iwanaka et al. (2005) proposed a new method for measuring wave height and direction with centimeter accuracy using a single commercial-grade GPS receiver on a buoy. By applying a high pass filter to GPS-based buoy data, they were able to extract the movement of a GPS-equipped buoy excited by ocean waves while minimizing the positioning error. Hou et al. (2006) applied the velocity integration method (VI-GPS) to measure wave direction using buoys, opting for VI-GPS over kinematic GPS positioning because kinematic GPS restricts the buoy's distance from the reference station. Nagai et al. (2008) used two sets of GPS buoys to observe wave climate, abnormally high waves, and offshore astronomical tides. Colbert (2010) conducted a cross-comparison of Datawell accelerometer buoys, Datawell GPS buoys and prototype GPS buoys to determine the viability of using off-the-shelf GPS receivers to measure ocean waves, finding good agreement between off-the-shelf GPS buoys, the newer Datawell GPS buoys and the traditional Datawell accelerometer buoys in the energetic part of the wave spectrum. Bender et al. (2010) showed there is very good agreement between GPS precise point positioning, GPS post-processed kinematic positioning and accelerometer measurements of wave height, peak period, and mean period. Doong et al. (2011) presented a methodology to derive wave parameters (e.g., significant wave heights, wave periods, wave direction, and wave spectrum) from GPS output velocities.

There are, however, some disadvantages with the methods presented above. The kinematic GPS positioning method is highly accurate but this method requires a fixed reference point and, therefore, the distance between the GPS buoy and base station is restricted (although it should be noted that in the post-processing mode of kinematic GPS positioning, centimeter-scale accuracy can be achieved for baseline up to 100 km). The DGPS method of wave measurement also requires an additional GPS reference station on shore, similarly restricting it to near-shore applications. Because of the restrictions of kinematic GPS positioning and DGPS, some researchers have used a velocity-integration method to get the precise velocity of GPS buoys and then used that velocity to estimate the position of the buoys (e.g. Doong et al. (2011)). However, this calculation requires the satellite velocity and can therefore only be used for non-real-time analysis; in operational systems, real-time computation is necessary. The method of Iwanaka et al. (2005) can measure wave parameters to high accuracy and does not have the restrictions of the other methods. In addition, its accuracy is also independent of GPS signal processing methods and the type of GPS observation made. The main limitation of this method is that it is based on high-pass filtering and selection of a cut-off frequency for the filter.

In this study, we use the method first proposed by Iwanaka et al. (2005) with the main focus being to present a procedure for selecting a reasonable cut-off frequency based on root mean square (RMS) differences in GPS height. The goal of this procedure is to allow measurement of ocean-surface waves to proceed from the

processing of data from a single GPS receiver, removing distance constraints between the GPS buoy and its base station and thus allowing GPS buoy placement even in the middle of the ocean. The input for our study is the observed GPS data collected from a wave simulator in a laboratory and then on a moored-sea GPS buoy. We use an algorithm that is based on the assumption that errors in GPS data are largely removed by a high-pass filter.

2. Key Concepts for Ocean Waves

2.1. Wave Height and Period

There are two parameters that are commonly used as indicators of the state of a given wave: wave height and wave period. The International Association of Hydraulic Research (IAHR) (1986) recommends that the wave height parameter of a surface wave in the time domain be defined by zero-crossing analysis, which is widely used to define both wave height and period. In the time domain, a wave period is defined as the time between a given direction of zero-crossing (a down-crossing or up-crossing) to the subsequent zero-crossing in the same direction.

Wave height is the difference between the maximum and minimum surface elevation of water in the relevant wave (Liu and Frigaard 1999). Different conventions have different definitions of wave height, however, depending on whether the trough is considered to occur after or before the crest. According to the Permanent International Association of Navigation Congresses (PIANC), waves are often defined as existing between two successive minima (Van der Burgt, 1994). This is similar to the IAHR (1986) definition. For this reason, waves are defined by down-crossings of zero in this paper, and this convention is used to determine the properties of waves.

Maximum wave height (H_{max}) is the largest crest-to-adjacent-trough value in the record, and is determined by (Liu and Frigaard, 1999):

$$H_{max} = \left[\sqrt{\ln N} + \frac{0.2886}{\sqrt{\ln N}} \right] H_{rms} \qquad (1)$$

where H_{rms}, is

$$H_{rms} = \left[\frac{1}{N} \sum_{i=1}^{N} H_i^2 \right]^{1/2} \qquad (2)$$

and N is the number of individual wave height measurements in the record. The average wave period ($\bar{T}_z$) is determined by (Liu and Frigaard, 1999):

$$\bar{T}_z = \frac{T_s}{N_z} \qquad (3)$$

where N_z is the number of zero-crossings and T_s is the total duration of the measurement.

2.2. Wave Direction

Directional measurements of the wave field made by floating buoys provide the time series

$$X(t) = \{X_1(t), X_2(t), X_3(t)\} \qquad (4)$$

where t is time and the subscript "1" refers to the vertical displacement, while "2" and "3" refer to the displacements in the east and north directions, respectively. The correlation functions of these displacements are defined as follows,

$$A_{mn}(\tau) = \lim_{x \to \infty} \frac{1}{T} \int_{-T/2}^{T/2} X_m(t)X_n(t+\tau)dt, \ m, n = 1, 2, 3, \cdots \qquad (5)$$

where τ is the time lag. Cross spectra are derived from the Fourier transform of Eq. (5),

$$C_{mn}(\omega) = K_{mn}(\omega) + iQ + mn(\omega) = \int_{-\infty}^{\infty} A_{mn}(\tau)e^{-i\omega\tau}d\tau \qquad (6)$$

where ω is the frequency, i is the standard imaginary unit, and K and Q are real numbers. Because the movement of a buoy is circular, the phase difference between X_1 and X_2 and between X_1 and X_3 is 90°, and the phase difference between X_2 and X_3 is 0° or 180°. We then have the following Eq.:

$$K_{12} = K_{13} = Q_{23} = 0 \qquad (7)$$

After substitution of Eq. (7) into Eq. (6), we arrive at

$$C_{12} = iQ_{12}, \ C_{13} = iQ_{13}, \ C_{23} = iK_{23},$$
$$C_{11} = \phi_1, \ C_{22} = \phi_2, \ C_{33} = \phi_3 \qquad (8)$$

where ϕ_1, ϕ_2, ϕ_3 denote the power spectrum of the wave in each axis, and ϕ_1 in particular is the power spectrum of the wave ϕ. The spectral resolution of ocean wave energy can be expressed by multiplication of the power spectrum $[\phi(\omega)]$ and its direction distribution function $[G(\omega, \theta)]$ (Huang et. al., 1998):

$$S(\omega, \theta) = \phi(\omega)G(\omega, \theta) \qquad (9)$$

where θ is the direction of the wave relative to the north. Each function has following relationships:

$$\phi(\omega) = \int_0^{2\pi} S(\omega, \theta)d\theta \quad \text{and} \quad \int_0^{2\pi} G(\omega, \theta)d\theta = 1$$

The direction distribution function can be expanded as a Fourier series:

$$G(\omega, \theta) = \frac{1}{2}a_0 + (a_1 \cos\theta + b_1 \sin\theta)$$
$$+ (a_2 \cos 2\theta + b_2 \sin 2\theta) + L \qquad (10)$$

where L stands for the rest of the Fourier series. Longuet-Higgins et al. (1963) showed that the first four Fourier coefficients can be used to approximate the direction distribution function. The Fourier parameters in Eq. (10) and the cross spectra in Eq. (8) have the following relationships:

$$a_1 = \frac{Q_{12}}{\phi_1}, \quad b_1 = \frac{Q_{13}}{\phi_1}, a_2 = \frac{\phi_2 - \phi_3}{\phi_2 + \phi_3}, \quad b_2 = \frac{2K_{23}}{\phi_2 - \phi + 3} \qquad (11)$$

Using this, we can then calculate the direction distribution function from the cross spectra. The wave direction is defined as the direction in which $G(\omega, \theta)$ has the greatest value $\bar{\theta}(\partial G/\partial\theta = 0)$:

$$\bar{\theta} = \tan^{-1}\frac{b_1}{a_1} = \tan^{-1}\frac{Q_{13}}{Q_{12}} \qquad (12)$$

The wave direction estimated in this study is calculated at the frequency ω that has the greatest power spectra (see Iwanaka et al. 2005).

3. Errors in GPS Measurements and High-Pass Filtering

Several kinds of errors and biases contaminate GPS measurements. These can be classified as satellite-dependent errors, signal propagation-dependent errors and receiver-dependent errors. The errors originating at the satellites include satellite ephemeris and satellite clock errors. The signal propagation errors include ionospheric and tropospheric effects. The errors originating at the receiver include receiver noise, receiver clock errors, the multipath error and antenna phase center variations. Table 1 summarizes the errors present in GPS observations, and the expected time intervals over which the errors could be detected. All numbers are approximate values and are subject to variances. Altogether these factors equate to an error of ± 5.1 meters. This is in fact a minimum estimate of the error, because other variables such as the elevation angle of the satellite, the strength of the received signal, and the changing multipath environment must have not been taken into account (Kuusniemi, 2005).

There are several algorithms that can be used to increase the accuracy of GPS measurements such as differential GPS and real time kinematic positioning methods. Both of these methods require a fixed reference point, however, so GPS buoy positioning is restricted by the need to maintain a relatively small distance to the a base station.

Figure 1 shows a typical position result over one hour of measurements from a regular GPS receiver set on a buoy. These data were

VERSITA

Table 1. Expected characteristics of GPS system errors (Hofmann-Wellenhof *et al.*, 2007).

Error Source	Range (1σ *)	Time scale
Shifts in the satellite orbits	~2.1 m	~1 hr
Clock errors of the satellites' clocks	~2.0 m	~5 min
Ionospheric effects	~4.0 m	~10 min
Tropospheric effects	~0.5 m	~10 min
Multipath effect	~1.0 m	~100 s
Calculation and rounding errors	~0.5 m	White noise

* σ is the standard deviation of observations
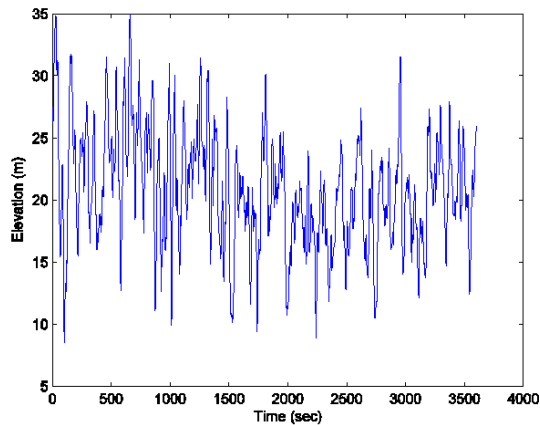
Figure 1. GPS Height data from the wave simulator collected during the laboratory experiment.

Figure 2. Power spectrum of the GPS height data from the wave simulator collected during the laboratory experiment (in m^2/Hz).

Figure 3. Part of perfect harmonic ocean wave motion (heaved wave) simulated by the laboratory simulator.

Figure 4. Power spectrum of the heaved wave data from the wave simulator in the laboratory experiment (in m^2/Hz).

generated in laboratory experiments using a dynamic simulator (see Fig. 6, next section). The power spectrum of the positioning data in Fig. 1 is shown in Fig. 2, demonstrating that almost all of the power in the GPS positioning data exists below 0.01 Hz. The laboratory simulator also provides an environment simulating perfect harmonic ocean wave motion, here called "heaved wave motion" (Fig. 3). Figure 4 shows the power spectrum of the heaved wave data simulated in this laboratory experiment; the data show an 11 s period and an energy peak located at 0.09 Hz. These characteristics mean that a suitably designed high-pass filter can extract the movement of a GPS-equipped buoy excited by ocean waves with minimum influence from GPS positioning errors. This is the key principle behind measuring ocean waves by GPS positioning. When the high pass filter is adopted, the mean value of the antenna's elevation becomes zero, but this is not a problem as we require only the rotational movement of the buoy, not its absolute elevation. Figure 5 shows the result of data filtered by a high pass filter with a cut-off frequency of 0.05 Hz (the original signal and its power spectrum are shown in Fig. 1 and 2 respectively). It looks non-periodic because the data have still GPS positioning errors.
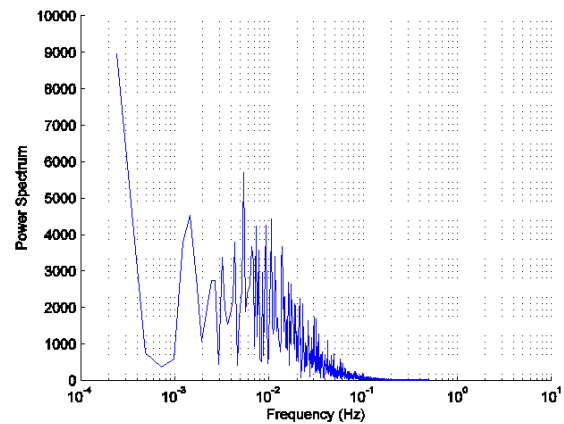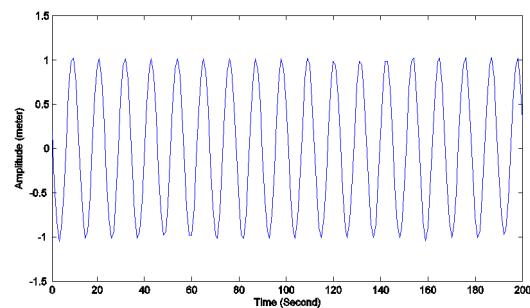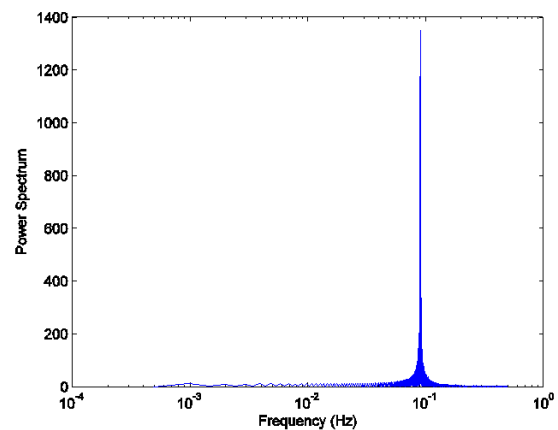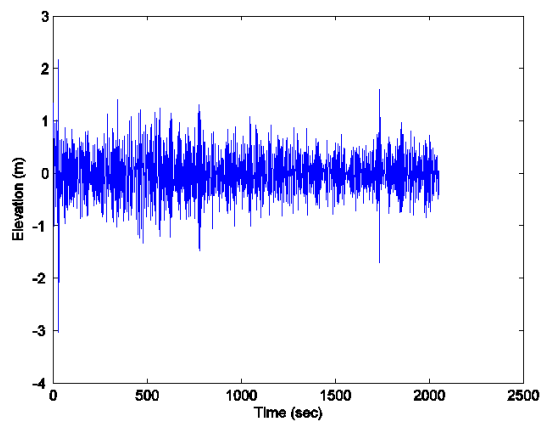
VERSITA

Figure 5. High-pass-filtered GPS height data from the wave simulator, with a 0.05 Hz cut-off frequency.

Figure 6. Schematic view of the dynamic simulator (courtesy Doong, 2011).

4. Numerical Investigations

We conducted laboratory experiments to test the concept of using a single GPS receiver and the software package developed in this study to determine wave motion parameters. The software package is written in MATLAB and is based on the zero down-crossing method to estimate the wave parameters (see Section 2.1): the wave height estimation by Eq. (1), and the wave period estimation by Eq. (3). Eq. (12) is used to estimate the wave direction. Before analyzing the GPS data for the wave parameters computation, we have used a simple high-pass filter algorithm on the GPS position data (see Section 3). This passes through high-frequency components of the GPS position data, while rejecting the low-frequency components in which most of the GPS error lies. The software package also includes a five-step procedure to find optimum cut-off frequency (see below).

A dynamic simulator (Fig. 6) was used to perform the experiments. It consists of a wave simulator and a GPS receiver. The wave simulator enables a uniform circular motion to be created in the vertical plane with a specific period. The simulator used in this study belongs to the Fugro OCEANOR AS, and is used for executing laboratory experiments. This simulator has a rotating arm to which a GPS receiver is fixed, simulating the motion of a buoy floating in the ocean. The arm of the simulator is 1.0 m long, such that the maximal vertical displacement is 2.0 m. The period of rotation is set to 11 seconds and the plane of motion of the arm lies 266° of true north. The GPS receiver used in the simulator is a Jupiter 21 (NAVMAN Inc.) model, and the GPS observations are single-point positioning as processed by GPS receiver's commercial software, output in NMEA format. The sampling rate is 1 Hz, and 90 minutes of data are recorded during the test run. Fig. 7 shows the results of this experiment, with processed GPS data shown in earth fixed Cartesian coordinates both before and after filtering. Before filtering, the coor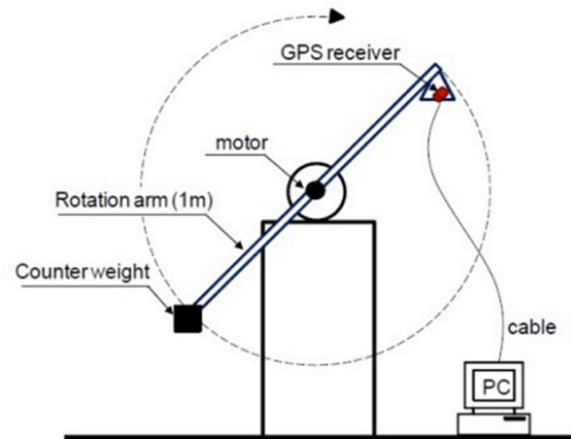dinate system must be transformed from latitude, longitude and height to an east, north and height local frame. The origin of the local frame is the initial position of the sensor (taken from GPS measurements) because knowledge of the absolute position is not necessary to obtain the rotational motion of the buoy (as shown in the three parts of Fig. 7, the systematic errors in the GPS system are present in the position data even though the wave simulator is not changing its position). It should also be noted that jumps may be seen in the GPS data that should be removed from the GPS position data: their large wavelengths become a problem when using the high-pass filter by changing the power spectrum of the position data. One simple way to remove the jumps is to remove the offset between the positions before and after each jump. There were not any jumps in the GPS data in this study.

After coordinate transformation and jump removal, the next step in GPS data processing is selecting the cut-off frequency for high pass filtering data. This stage is very important because there is very little signal in GPS data at frequencies higher than 0.01 Hz, so results will vary greatly depending on the cut-off frequency (see Table 2). We chose five different cut-off frequencies and computed wave parameters from each of these; our results justified our belief that the variability of the final parameters is dependent to the cut-off frequency. As an example, the arm of simulator (which is 2 m long) is calculated to be 1.87 m long when 0.034 Hz is chosen as the cut-off frequency. The best result is achieved with the frequency of 0.031 Hz, which leads to a calculated simulator arm length of 2.009 m. We also tested a new procedure to choose the cut-off frequency based on the root mean square (RMS) of the transformed GPS heights after returning from the frequency domain to the time domain, and after filtering. The RMS value of wave height is the square root of the mean of the squared values of all wave heights measured over a given interval. Most of the time, the wave height value is changing continuously and significantly, so it is not a good measure of the wave real effect. However, the RMS value is the ef-
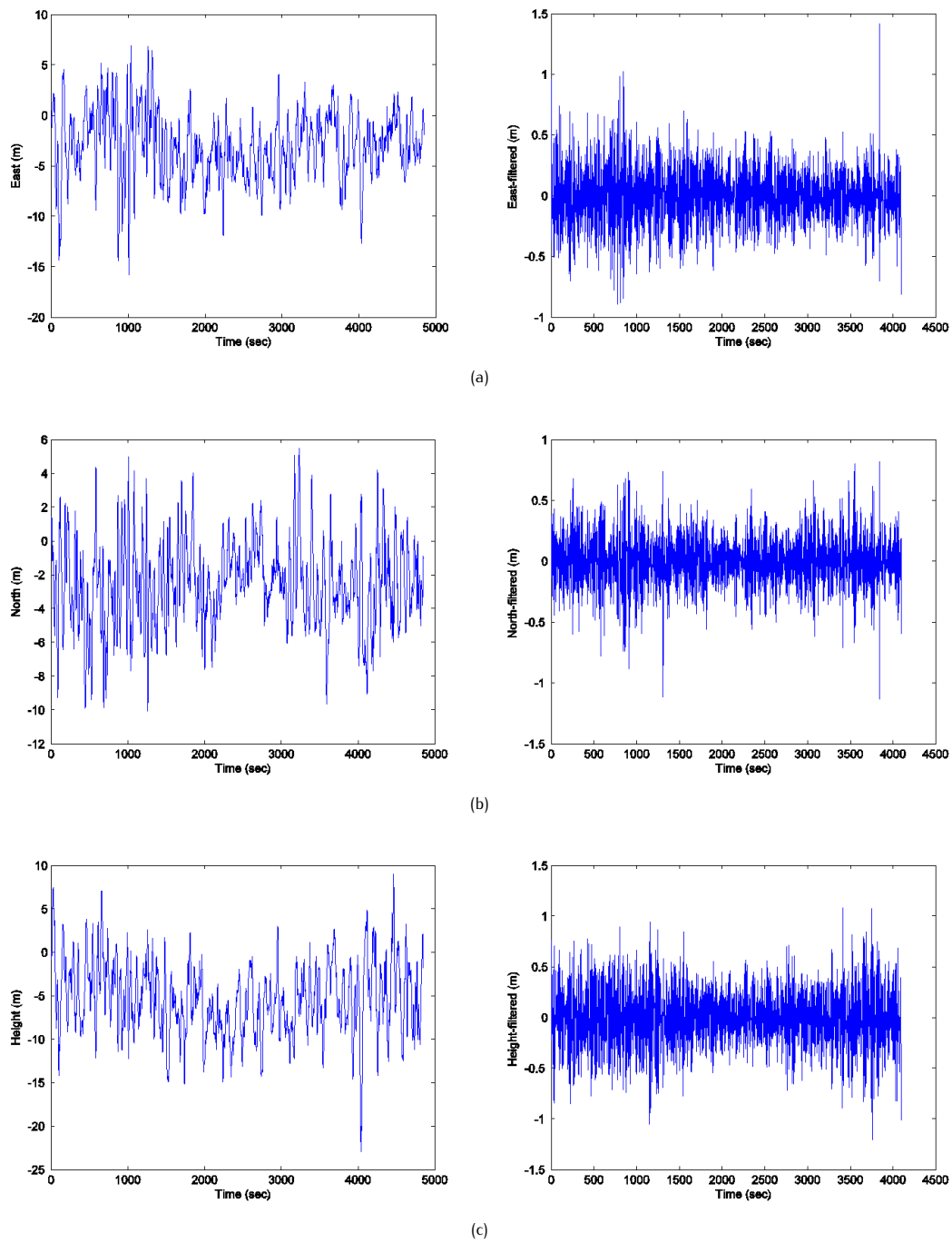
(a)

(b)

(c)

Figure 7. (a) East coordinate results of processed GPS data from the wave simulator in the laboratory experiment before (left) and after (right) filtering.(b) North coordinate results of processed GPS data from the wave simulator in the laboratory experiment before (left) and after (right) filtering.(c) Height coordinate results of processed GPS data from the wave simulator in the laboratory experiment before (left) and after (right) filtering.

Table 2. Wave parameters for the laboratory-simulated data using different cut-off frequencies for the high-pass filter.

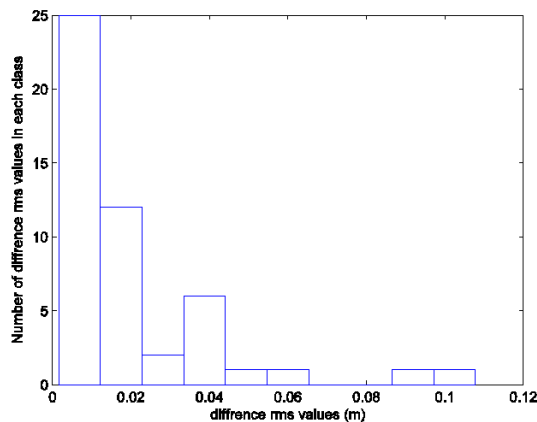| Frequency (Hz)	H_{max} (m)	$T_{average}$ (s)	Direction
0.030	2.09	14.05	256.6°
0.031	2.009	11.488	264.6°
0.032	1.873	12.47	264.5°
0.033	1.774	12.60	264.3°
0.034	1.866	11.33	264.0°

Figure 8. Histogram of root mean square (RMS) error in the GPS height data from the wave simulator in the laboratory experiment.

Figure 9. Directional wave spectrum of the simulated data in the laboratory experiment.

fective value of variation between waves, therefore, it is used as the criterion in our method. To use the RMS values as a criterion, the following steps are done: 1. Selection of cut-off frequencies from 0.01 to 0.05 Hz in steps of 0.001 Hz. (see Table 2 for sample choices of cut-off frequency) 2. Performance of high-pass filtering of the GPS height data in the frequency domain. 3. Transformation of the filtered data from frequency domain to the time domain. 4. Computation of RMS for the transformed data. 5. Computation of the RMS differences for the consecutive cut-off frequencies. Figure 8 shows the histogram of RMS differences for the simulated data. This figure is the basis for RMS criterion chosen in this study. As can be seen from Fig 8, the value of the RMS difference in the 0.001–0.01 Hz range is the highest for the whole sample. Because of this, we chose a value of 0.01 Hz such that the RMS difference for the consecutive cut-off frequencies becomes less than 0.01 Hz.

Using the above procedure, we arrived at a cut-off frequency for simulated data in the laboratory of 0.031 Hz, and were then able to filter the GPS height data and finally to compute wave parameters. The results are shown in Table 3. We set the period of rotation and the direction of the arm from the true North to known values, to compare against estimations derived from Eqs. 1, 3, and 12. Figure 9 shows the directional wave spectrum of the simulated data
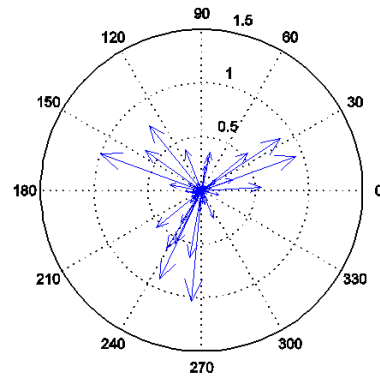
from which we calculated the wave direction with the frequency ω that has the greatest power spectrum, estimated using the cut-off frequency calculated for this experiment (0.031 Hz). Using different cut-off frequencies resulted in different spectra (see Table 2). The maximum wave height (in our experiment, the diameter of the arm's rotation) is calculated to be 2.009 m, a discrepancy of 9 mm from the true value, while the calculated wave period differed by 0.488 s from its true value and the discrepancy between calculated and true direction is 1.4°. These results show the accuracy possible using a single GPS receiver together with the RMS procedure for selecting the optimal cut-off frequency for a high-pass filter.

We also performed field test with a GPS receiver installed on a buoy moored along the coast of the An-Ping harbor in Tainan, Taiwan: a "moored-sea" field test that, it should be noted, does not quite match the type of signal produced by a wave in the middle of the ocean. The approximate deployed location of the buoy is 22° 58′43″ N, 120° 10′33″ E at a depth of −7.5 m. The buoy used in this study is of a simple, compact design that has been previously used to collect a time series of wave heights in a coastal area (e.g., Cheng et al., 2010). The buoy is built by attaching a geodetic-grade antenna (of a Javad Regant single depth chokering type) on top of a typical lifesaver buoy and then covering it with a fiberglass radome for waterproofing (Fig. 10). The buoy was tethered to the land with 30 m ropes, which were used to limit the horizontal location of the buoy without interfering in collection of buoy-height data, and also to prevent the buoy from moving to the channel of the harbor for security reasons. The ropes were not fully tensioned during most of the observation time since it was a relatively calm day. The rope should not have affected the buoy's vertical motion much since it was also afloat. The other end of the rope was tethered to the land, at about 1 m higher than the water level, such that the rope would have risen out of the water had the rope been under tension. A second rope on the same side of the buoy as

Table 3. Wave parameters estimated from GPS height data on the wave simulator in the laboratory experiment.

Parameter	Experiment result	True Value	Maximum bias of the derivation	Mean bias of the derivation	Minimum bias of the derivation
Wave height	2.009 m	2 m	0.226 m	0.18 m	0.009 m
Wave period	11.488 s	11 s	3.05 s	1.39 s	0.33 s
Wave direction	264.6°	266°	9.4°	3.2°	1.4°

the tide gauge was letting loose, so additionally the buoy would have rotated 90° counterclockwise had the other rope been tensioned. In summary, while there may have been external forces on the buoy due to the rope, the surveyors did their best to minimize those forces such that the data should still be credible. The sampling rate of the GPS buoy is 1 Hz. The time series of buoy heights was processed in the kinematic mode with respect to a reference station on land about 1.6 km away. The software Kinematic and Rapid Static (KARS), originally developed by the National Geodetic Survey (NGS) of the U.S., was used to process the GPS buoy data in the kinematic mode using L1/L2 carrier phases with a double-differencing technique.
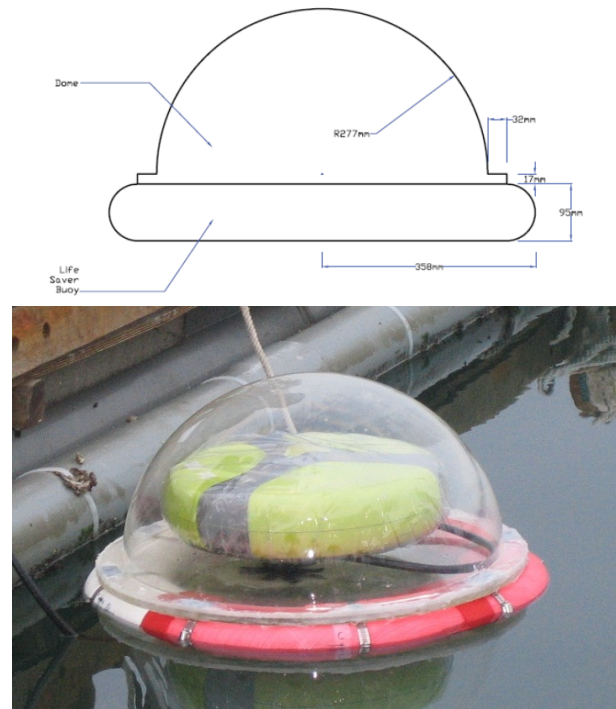
Data from the buoy were collected on April 2, 2008, and we used 120 minutes of GPS data in this analysis. The same procedure was carried out to estimate the wave parameters for moored-sea GPS buoy as for the laboratory simulation test. This included the five-step procedure to find the optimum cut-off frequency, which we estimated to be 0.011 Hz for the moored-sea GPS buoy. The processed GPS buoy data in components of Cartesian coordinates are shown in Fig. 11 and Fig. 12. The off-position points in Fig. 11 are because the moored GPS buoy is not completely fixed at a point, as described above. Table 4 shows the results of wave computation for GPS buoy data estimated using a cut-off frequency of 0.011 Hz based on the RMS criteria. Another study in the north-west coast of Taiwan resulted a wave height between 20 cm to 4 m over a two month period, and a wave period of 5–15 s or more at the same location (Hou, 1998), which is in good agreement with our results for the Taiwanese coastal area.

Figure 10. Diagram (top) and image (bottom) of the GPS buoy used at the Taiwanese coast (Cheng *et al.*, 2010).

Table 4. Wave parameters estimated from the moored-sea GPS buoy experiment.

Parameter	Result
Maximum Wave Height	17 cm
Average Wave period	18.78 s
Wave direction	226.5°

5. Conclusions

We applied a methodology to derive ocean wave parameters (wave height, wave period and wave direction) from GPS buoy data, and presented a method to reduce the error in these estimated wave parameters. The power spectrum of the GPS data (including its errors) and of the buoy's movement (excited by ocean wave) were the basis for the estimation of wave parameters. Because the buoy movement data is in a frequency band in the GPS data with a very low signal to noise ratio (SNR), the most important point in design of a high-pass filter was the selection of a cut-off frequency; because of this, we selected a cut-off frequency based on the root mean square (RMS) error in GPS-derived height data after transforming these data back to the time domain (from the frequency domain) after filtering. The estimated accuracy of the wave period, height and direction deviate significantly with changes in the cut-off frequency, but the RMS method used in this study provides a tool to reduce the error of the estimated wave parameters.

To verify our methodology, we performed a laboratory experiment consisting of a dynamic wave simulator with a GPS receiver at-
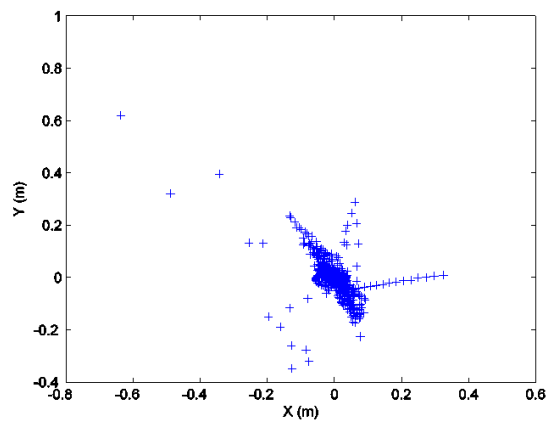
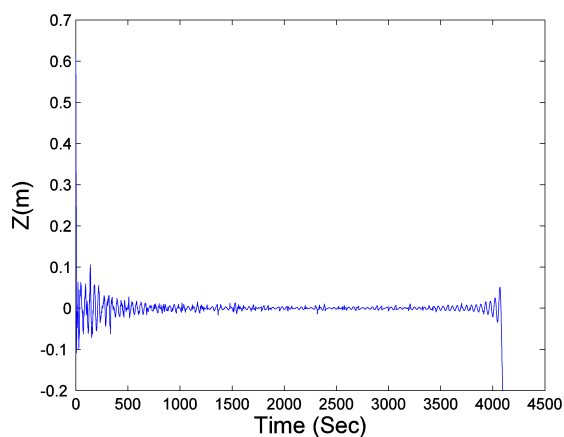**Figure 11.** Horizontal positions of moored-sea GPS buoy after filter-
ing.

Figure 12. Heights of moored-sea GPS buoy after filtering.

tached to it. This was used to simulate perfect harmonic ocean
wave motion. Results of wave computations with the selection of
the optimal cut-off frequency with RMS method showed an error
of the wave height computations at roughly 1%, and errors of 1%
and 5% in the wave direction and wave period estimations, respec-
tively. We also estimated the directional wave spectrum and used
this to calculate the wave direction to achieve the greatest power
spectrum. A moored-sea buoy test was also performed to test our
method in more realistic conditions, because there were no other
buoy data available for this project in the region in which we per-
formed the moored-sea test. Therefore, we performed the lab ex-
periment as the validation test for our moored-sea investigation.
Our results agree well with those reported by Hou (1998) at the
same test area, both for wave height and wave period.

Use of a single GPS receiver to measure wave parameters does not
require complicated processing to extract wave data, but can be
done simply with the application of a high-pass filter to the GPS
point-positioning data. Therefore, the algorithm described here
can be executed in the navigation processing core of any GPS re-
ceiver. Using this method enables us to reduce the amount of
data transmitted from sensors to a land station via communica-
tion satellites in other words, it is possible to avoid transmitting raw
GPS data for processing, instead transmitting only analyzed ocean
wave data. Because of this, the method proposed here reduces not
only the price of a sensor system but also its operating cost.

References

Bender L. C., Howden S. D., Dodd D. and Guinasso N. L., 2010,
Wave Heights during Hurrincane Katrina: An Evaluation of PPP
and PPK Measurements of the Vertical Displacement of the
GPS Antenna, J. Atmos. Oceanic Tech., 27, 1760-1768.

Cheng K. C., Kuo C. Y., Tseng H. Z., Yi Y. and Shum C. K.,
2010, Lake surface height calibration of Jason-1 and Jason-2
over the Great Lakes, Mar. Geod., 33 (S1), 186–203.

Colbert D., 2010, Field Evaluation of Ocean Wave Mea-
surements with GPS Buoy, NAVAL Postgraduate School.

De Vries J. J., Waldron J. and Cunningham V., 2003, Field
tests of the new Datawell DWR-G GPS wave buoy, Sea Tech-
nol., 44, 50-55.

Doong D. J., Lee B. C. and Kao C. C., 2011, Wave Measure-
ments Using GPS Velocity Signals, Sensors, 11, 1043-1058.

Hofmann-Wellenhof B., Lichtenegger H. and Walse E., 2007,
GNSS- Global Navigation Satellite Systems, GPS, GLONASS,
Galileo, and more, SpringerWienNewYork.

Hou H. S., 1998, Study of Shelf Waves vs. Sand drifts in
NW coast of Taiwan, Proceeding of the international Confer-
ence on Coastal Engineering, No. 21, 1152- 1166.

Hou D., Hamada M., Yoo Y. and Kouguchi N., 2006, Evalu-
ation Test Result on Wave Direction Measurement Using GPS

VERSITA

Buoy, Proceeding of the Ocean's 06 Asia Pacific IEEE.

Huang M. C. and Chen J. Y., 1998, Wave Direction Analysis from Data Buoys, Ocean Eng., Vol. 25, No. 8, 621-637.

International Association of Hydraulics Research (IAHR), 1986, List of sea parameters.

Iwanaka Y., Kasai T., Murayama T., Harigae M., Yamaguchi I., Nakanishi H., Suko H. and Igawa H., 2005, Abreast of the waves: Moored-sea sensor to measure height and direction, GPS World. 2005, 16, 16-27.

Jeans G., Bellamy I., de Varies J. J. and van Weer P., 2003, Sea Trial of the New Datawell GPS Directional Waverider. Fugro GEOS Ltd., Swindon, UK Current Measurement Technology, Proceeding of the IEEE/OES Seventh Working Conference, 145-147.

Krogstad H., Barstow S., Aasen S. and Rodriguez I., 1999, some recent development in wave buoys measurement technology, Coast Eng., 37, 309-329.

Kuusniemi H., 2005, User-level reliability and quality monitoring in satellite-based personal navigation. PhD dissertation, Institute of Digital and Computer Systems, Tampere University of Technology, Finland.

Liu Z. and Frigaard P., 1999, GENERATION AND ANALYSIS OF RANDOM WAVES, Aalborg University.

Longuet-Higgins M. S., Cartwright D. E. and Smith N. D., 1963, Observations of the directional spectrum of sea waves using the motions of a floating buoy, Ocean Wave Spectra., 111- 136.

Nagai T., Shimizu K., Sasaki M. and Murakami A., 2008, Characteristics of the Observed Offshore Wave Data by the GPS Buoys, Proceeding of the Eighteenth International Offshore and Polar Engineering Conference.

Van der Burgt C., 1994, Permanent International Association of Navigation Congresses (PIANC), Marine Pollution Bulletin, Vol. 29, Nos 6-12, pp. 398-400.

VERSITA